

# Deformed halo nuclei probed by breakup reactions

**Takashi Nakamura**

Department of Physics, Tokyo Institute of Technology, 2-12-1 O-Okayama, Meguro, Tokyo  
152-8551, Japan

E-mail: [nakamura@phys.titech.ac.jp](mailto:nakamura@phys.titech.ac.jp)

**Abstract.** Breakup reactions play important roles in elucidating the structures near the drip lines, such as nuclear halo. The recent experimental results using the Coulomb and nuclear breakup reactions for the neutron-drip-line nuclei at the new-generation RI beam facility, RIBF at RIKEN, are presented. Focuses are put on the results on the newly found halo nucleus  $^{31}\text{Ne}$ , which is intriguing also in that this nucleus is in the island-of-inversion and thus could be strongly deformed. The results on other Ne/Mg/Si neutron rich isotopes ranging from  $N=20$  towards  $N=28$  are also briefly reported. The first breakup experiments using SAMURAI facility at RIBF and future perspectives are also presented.

## 1. Introduction

Structural Evolution of atomic nuclei towards the neutron and proton drip lines in the nuclear chart is one of the most important and intriguing issues in current nuclear physics. In particular, the location of the neutron drip line is the key to understand the stability of atomic nuclei around the bound limit of neutron-proton quantum system. In spite of such importance, the neutron drip line has been determined only up to the oxygen isotopes. The drip-line nuclei exhibit peculiar feature of nuclear structures as in neutron halo nuclei found in the vicinity of the neutron drip line. However, the neutron halo nuclei so-far known have been limited to the light system, and the heaviest neutron halo nucleus experimentally known had long been  $^{19}\text{C}$  [1]. The  $1n$  halo nucleus  $^{31}\text{Ne}$  [2] and the  $2n$  halo nucleus  $^{22}\text{C}$  [3], heavier than  $^{19}\text{C}$ , have been identified only very recently. In what region and how the heavier halo nuclei can be formed are key questions in discussing the nuclear structure near the drip line.

It has been established that the shell is evolving from the stability line towards the neutron drip line. One of highlights of such phenomena is the island of inversion for the neutron-rich nuclei near  $N \sim 20$  [4], where the ground state becomes dominated by the intruder configuration. The island contains the strongly deformed  $^{32}\text{Mg}$  [5] and neighboring Ne/Na/Mg [6, 7, 8] isotopes. Theoretically, the shell model also shows such an island [4, 9, 10]. Note also that the loosely-bound feature enhances the shell evolution. The interplay between the halo formation and the shell evolution could thus be studied at the neutron-rich edge the island of inversion.

The neutron-rich nuclei with neutron number  $20 < N < 28$  in the island of inversion can indeed provide us with some insights about the shell evolution and the halo phenomena. The halo is formed on the condition that the nucleus has a very small  $1n$  or  $2n$  separation energy ( $S_n, S_{2n} < 1$  MeV), and that the least bound neutron has low or no angular momentum,  $s$  or  $p$ . The latter condition is not met for nuclei with  $20 < N < 28$  if we adopt the conventional shell order since the least bound neutron in  $0f_{7/2}$  moves with a large centrifugal barrier. On



the other hand, Utsuno and Otsuka et al. predicted the effective single particle energy (SPE) between  $1p_{3/2}$  and  $0f_{7/2}$  becomes small or inverted for neutron-rich nuclei for  $Z \sim 10$  [10], which may make the  $p$ -wave configuration dominant.

As was pointed out by Hamamoto [11], nuclei with neutrons in the nearly degenerate  $f_{7/2}$  and  $p_{3/2}$  shells, which couple strongly to each other by quadrupole-quadrupole interaction, can be quadrupole deformed. This could be one cause of the island of inversion. The one-particle motion in a deformed potential (Nilsson picture) also provides insights about such nuclei. The weakly-bound neutron has also an interesting behavior. Namely, the lower  $\ell$  configuration becomes dominant when  $S_n$  approaches zero [12, 13, 14]. For instance, the Nilsson orbit of  $[330]1/2^-$  is occupied by  $f_{7/2}$  neutron if  $S_n$  is deeper than about 3 MeV, while  $p_{3/2}$  becomes dominant below this energy.

In general, in heavier nuclei, least-bound neutron(s) may tend to occupy orbitals with higher angular momentum, which hinders the halo formation. On the other hand, if the shell evolution occurs, the deformation is developed, and the dominance of  $s$  or  $p$  orbital becomes significant, then the halo structure may be abundant along the neutron drip line from light to heavy nuclei. Two neutron halo in heavier nuclei is also intriguing since the two halo neutrons may be strongly correlated in space, called dineutron, as predicted by Migdal [15]. Hence, the understanding of the formation of halo in heavier drip-line nuclei is very important in current nuclear physics.

This paper reports the recent experimental study of the neutron rich B/C/Ne/Mg/Si isotopes by Coulomb and nuclear breakup reactions RIBF around 240 MeV/nucleon, in order to investigate the halo structure and single particle configuration of exotic nuclei. Main focus here is  $^{31}\text{Ne}$ , which has  $N=21$ . The part of the result is in Refs.[2, 16]

## 2. Breakup reactions of exotic nuclei

One of the important experimental probes for nuclei far from the stability is breakup reactions at intermediate/high energies. Because the Fermi level of drip-line nuclei lies close to the continuum, weakly bound levels can be easily excited to the continuum, which corresponds to breakup reactions. The breakup reactions thus play important roles since the cross section is significantly large for such nuclei, and is sensitive to the wave function of the least-bound nucleon(s). The breakup reaction shows very different characteristics, depending on the target [17, 18]. A heavy target such as Pb induces primarily Coulomb breakup, while a light target such as C induces nuclear breakup.

The Coulomb breakup can extract the  $E1$  response of the nucleus since it is essentially the photo absorption process. The Coulomb breakup cross section is written as,

$$\frac{d\sigma(E1)}{dE_x} = \frac{16\pi^3}{9\hbar c} N_{E1}(E_x) \frac{dB(E1)}{dE_x}, \quad (1)$$

where  $N_{E1}(E_x)$  denotes the number of the virtual photons for the electric dipole transition with the excitation energy  $E_x$  [19]. Such simplicity that the cross section can be factorized allows us to extract the  $E1$  strength distribution.

One of the important and unique features of halo nuclei is the strong enhancement of the electric dipole strength ( $B(E1)$ ) just above the neutron decay threshold, which we call soft  $E1$  excitation. This excitation is contrast to the  $E1$  response of normal nuclei near the stability, whose  $E1$  strength is concentrated almost fully on the Giant Dipole Resonance (GDR) at high excitation energies of about 20 MeV. Recently, another dipole excitation at lower excitation energies, called pygmy dipole resonance (PDR) has been observed for  $^{132}\text{Sn}$  [20]. It should be noted that the soft  $E1$  excitation and PDR has different characteristics in that the former is non-collective excitation, while the latter is considered to be collective. The PDR peaks at around  $E_x \sim 8\text{-}10$  MeV, higher than the soft  $E1$  excitation but lower than the GDR peak.

The mechanism of the soft  $E1$  excitation has been understood well for the  $1n$ -halo nuclei as the revelation of the direct breakup. In direct breakup mechanism, the  $E1$  response reflects the halo spatial distribution [21, 22, 23]. There, the matrix element is simply written as

$$\frac{dB(E1)}{dE_{\text{rel}}} = |\langle \Phi_f(\vec{r}, \vec{q}) | e_{\text{eff}}^{E1} \hat{T}(E1) | \Phi_i(\vec{r}) \rangle|^2, \quad (2)$$

where  $\Phi_i(\vec{r})$  and  $\Phi_f(\vec{r}, \vec{q})$  show the wave function of the ground state (halo state), and the final state in the continuum of the neutron relative to the core, respectively.  $\vec{r}$  is the relative coordinate of the neutron relative to the c.m. of the core.  $\Phi_f(\vec{r}, \vec{q})$  is also a function of the relative momentum  $q = \sqrt{2\mu E_{\text{rel}}/\hbar}$ . The electric dipole operator is  $\hat{T}(E1) (= rY^{(1)}(\Omega))$ . This formula shows that the  $B(E1)$  spectrum is approximately the Fourier-Bessel transform of the radial wave function of the ground state. This suggests that the large amplitude in the radial wave function at large  $r$  as in the halo state causes the large  $E1$  amplitude at small  $q$ , or small  $E_{\text{rel}}$  (relative energy) in the  $B(E1)$  spectrum. Note that the  $E1$  operator involving  $r$  causes further amplification [24]. This characteristics makes the soft  $E1$  excitation a very sensitive tool to probe the halo wave function as applied successfully to  $^{11}\text{Be}$  [21, 22, 23],  $^{15}\text{C}$  [25, 26], and  $^{19}\text{C}$  [1].

The soft  $E1$  excitation of two neutron halo nuclei is much more complicated, but has intriguing aspects. The current understanding for two-neutron halo cases is also non-resonant origin, but the initial two-neutron correlation and the final state interaction affect largely the  $E1$  spectra. It should be noted that for two-neutron halo nuclei, integrated sum of the low-energy  $E1$  strength reflects the spatial correlation [27, 28]. In Ref.[28], the dineutron correlation, which is a strong spatial  $nn$  correlation and has a mixture of different parity configurations, for the halo neutrons in  $^{11}\text{Li}$  is suggested, which is responsible for the strong  $E1$  strength of this nucleus.

Nuclear breakup of an unstable nucleus with a light target at intermediate/high energies offers a useful spectroscopic tool as well. The momentum distribution of the core fragment after  $1n$  removal can be used to extract the orbital angular momentum of the removed neutron, as demonstrated recently even for the unbound final state [29]. When a measurement is combined with that of the  $\gamma$  ray emitted from the core fragment, the core configuration of the projectile with the spectroscopic factor  $C^2S$  can also be extracted. For instance, when we study the  $1n$  removal of  $^{31}\text{Ne}$  into  $^{30}\text{Ne}$ , then the momentum distribution of  $^{30}\text{Ne}$  can probe the angular momentum of the neutron removed. When the  $\gamma$  ray emitted from the  $^{30}\text{Ne}$  core fragment is measured in coincidence, one can determine the ratio of  $^{30}\text{Ne}$  ground state configuration to the excited one. A combined analysis of Coulomb and nuclear breakup further enhances this capability due to different sensitivities to the spatial distribution of the wave function around the surface of exotic nuclei.

### 3. Inclusive Coulomb and nuclear breakup of neutron rich C/Ne/Mg/Si isotopes

In the Coulomb breakup, the  $E1$  energy spectrum characterizes the soft  $E1$  excitation, as mentioned above. A kinematically complete measurement of the breakup reaction, where the four-momentum vectors of the outgoing particles are measured in coincidence, is required to extract the excitation energy on event-by-event basis. The experiment is rather complicated where neutron(s) and charged fragments at relativistic energies should be measured in coincidence. Although such a measurement is possible within current experimental techniques, an alternative inclusive measurement, where only the integrated  $-1n(-2n)$  cross section is measured, has often advantage over the kinematically complete one, in that the experiment is simpler and no measurement for the neutron is required. Such a measurement is in particular important at the earlier stage of the new facility, as in that of the new-generation RI beam facility, RIBF, at RIKEN.

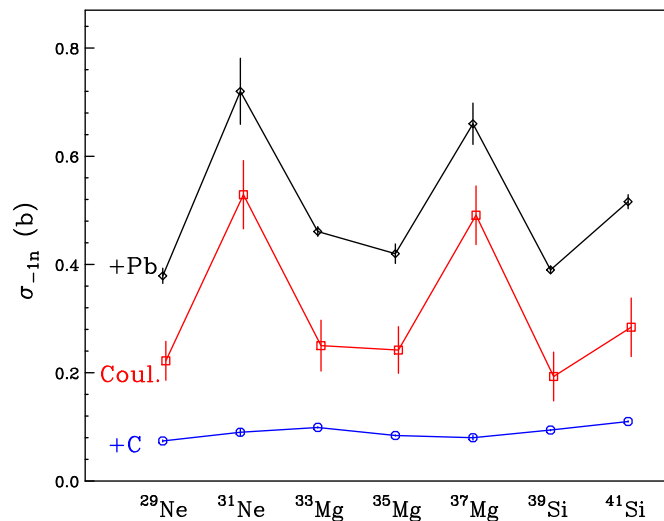


**Figure 1.**  $1n$  removal cross sections of  $^{29,31}\text{Ne}$ ,  $^{33,35,37}\text{Mg}$ , and  $^{39,41}\text{Si}$  on C (blue circles) and Pb (black diamonds) at 220-240 MeV/nucleon. The Coulomb breakup cross sections on Pb (red squares) are estimated by subtracting the nuclear breakup contribution estimated from the ones with the carbon target. The enhancement of the Coulomb breakup cross section is clearly seen for  $^{31}\text{Ne}$  and  $^{37}\text{Mg}$ .

The inclusive measurement, although it provides less information about the structure, has signature on the soft  $E1$  excitation. The inclusive Coulomb breakup cross section corresponds to measure the integrated cross section as shown in

$$\sigma(E1) = \int_{S_n}^{\infty} \frac{16\pi^3}{9\hbar c} N_{E1}(E_x) \frac{dB(E1)}{dE_x} dE_x. \quad (3)$$

The expression shows that the cross section is basically the integration of  $dB(E1)/dE_x$  weighted by the photon number  $N_{E1}(E_x)$  over the excitation energy. As the photon spectrum falls exponentially with  $E_x$  [2, 17],  $\sigma(E1)$  becomes significant only when the  $B(E1)$  is concentrated at low excitation energies as in the case of soft  $E1$  excitation for halo nuclei. In fact, it can be estimated that for  $^{31}\text{Ne}$  the cross section of about 0.5 b is expected when it is a halo nucleus that causes a soft  $E1$  excitation, while the GDR contributes only about 0.06 b [17]. It should be noted that for a  $1n$  plus core system, the upper limit of the integration could be limited to  $E_x \sim S_{2n}$  since above that the nucleus decays into  $2n$ +fragment when the measurement requires only  $-1n$  channel. With that the GDR contribution will become negligible. Hence the soft  $E1$  excitation can even be more easily distinguished.

The inclusive breakup cross sections ( $1n$  and/or  $2n$  removal cross sections) of  $^{19,20,22}\text{C}$ ,  $^{29,31}\text{Ne}$ , and  $^{33,35,37}\text{Mg}$  at 220-240 MeV/nucleon have been measured at ZDS (Zero Degree Spectrometer) at the next-generation RI beam facility, RIBF, at RIKEN [2, 16]. The  $1n$  removal cross sections for Ne, Mg, and Si isotopes are shown in Fig. 1.

As shown, the cross section for  $^{31}\text{Ne}$  and  $^{37}\text{Mg}$  among others are significantly larger ( $\sim 0.5$  b), expected for the halo nucleus. As detailed in Ref. [2], the nucleus  $^{31}\text{Ne}$  has been identified as a new  $1n$  halo nucleus, evidenced by this enhanced Coulomb breakup cross section.

We can further investigate the structure of these nuclei by using the combinatorial analysis of nuclear and Coulomb breakup. The preliminary analysis combined with the  $\gamma$  ray coincidence shows the rather small ground-state  $^{30}\text{Ne}$  core configuration ( $\sim 30\%$ ) with small  $S_n$  of about

100 keV with  $J^\pi=3/2^-$ . The result is well compatible with the large scale shell model, which predicts such ground state spin-parity. The shell model also shows the large configuration mixing of  $^{30}\text{Ne}(0_1^+) \otimes \nu 1p_{3/2}$ ,  $^{30}\text{Ne}(2_1^+) \otimes \nu 1p_{3/2}$ , and  $^{30}\text{Ne}(2_1^+) \otimes \nu 0f_{7/2}$ , which is also consistent with the preliminary result of the momentum distribution of  $^{30}\text{Ne}$ .

Such a configuration mixing can be regarded as the development of the deformation. Hamamoto [14] describes the valence neutron of  $^{31}\text{Ne}$  lies in the Nilsson orbit  $[330]1/2^-$  or  $[321]3/2^-$ . More recently, the ground state properties of  $^{31}\text{Ne}$  were also discussed using the particle-rotor model, which takes into account the rotational excitation of the  $^{30}\text{Ne}$  core [30]. Since the mean field potential is quadrupole deformed, which causes the configuration mixing involving  $p$ -wave in  $^{31}\text{Ne}$ , we may call such a system “deformed halo nucleus”. Our preliminary analysis also finds that the structure of the deformed core plus  $p$ -wave halo neutron also takes place for  $^{37}\text{Mg}$ . Such a halo system could be common in the neutron-drip part of the island of inversion region.

#### 4. Breakup reaction experiments at SAMURAI facility

As mentioned, ideally, the breakup reaction should be measured in complete kinematics. With that, in the Coulomb breakup one can map  $B(E1)$  as a function of the excitation energy with the aid of Eq. (1). Note that the  $B(E1)$  distribution contains information of the ground state wave function, such as  $C^2S$  (spectroscopic factor),  $\ell$  (orbital angular momentum), and  $S_n$  (separation energy) of the halo state. The kinematically complete measurement is also a suitable tool to study the dineutron correlation.

The SAMURAI (**S**uperconducting **A**nalyser for **M**ulti-particles from **R**adio **I**sotope **B**eams) has been constructed to realize such kinematically complete measurement with high efficiency and with the intense RI beam available at RIBF. SAMURAI comprises the superconducting magnet with a maximum magnetic field of 3.1 Tesla ( $B_{max}L=7.1$  Tm), beam detectors, heavy ion detectors, and the neutron detector array NEBULA (**N**eutron-detection system for **B**reakup of **U**nstable nuclei with **L**arge **A**cceptance).

The SAMURAI facility has successfully commissioned in March, 2012, followed by the day-one campaign experiment in May, 2012, using the  $^{48}\text{Ca}$  beam at 345 MeV/nucleon, which includes the kinematically complete measurement of Coulomb breakup of two neutron halo nuclei  $^{19}\text{B}$  and  $^{22}\text{C}$ . We had the beam intensity of  $\sim 100$  counts per second (cps) for  $^{19}\text{B}$  and of  $\sim 15$  cps for  $^{22}\text{C}$ , about 3-4 orders of magnitude larger than those obtained in the previous facility (RIPS). These nuclei are considered to be important in understanding the dineutron correlation of the  $2n$  halo systems. The  $^{22}\text{C}$  could be the last  $s$ -wave dominant two neutron halo system that the current, and near-future-planned experimental facilities can reach. In SAMURAI, we also plan to study the deformed halo nuclei in kinematically complete measurements in the near future. We expect that the mechanism of the revelation of such system will be clarified soon.

#### 5. Summary

The importance and usefulness of the breakup reactions at intermediate/high incident energies in the new-generation RI beam facility has been demonstrated. Inclusive breakup measurements at the new-generation RI beam facility, RIBF at RIKEN, were briefly presented, where evidence for the  $1n$  halo structure in  $^{31}\text{Ne}$  is shown. The large configuration mixing suggested from the combined analysis of Coulomb and nuclear breakup reactions and the large scale shell model calculation indicates that the  $^{31}\text{Ne}$  is a deformed halo nucleus, where  $p$ -wave neutron is orbiting the deformed core potential. Such a unique system is also suggested for  $^{37}\text{Mg}$ .

The new facility SAMURAI at RIBF, which aims at conducting the kinematically complete measurements of breakup reactions of very neutron-rich nuclei, has commissioned in 2012. The first series of physics experiments, one of which is the kinematical complete measurement of the Coulomb breakup of  $^{19}\text{B}$  and  $^{22}\text{C}$  at about 240 MeV/nucleon, have been successfully performed.

This demonstrates the powerfulness of the facility, so that we expect that such breakup reactions are applied to more exotic and heavier nuclei along the drip lines in the near future, including the deformed halo nuclei near  $N=20$  and  $N=28$ .

### Acknowledgments

The author would like to thank the collaborators of the  $^{31}\text{Ne}$  experiment [2]. The author also would like to thank the SAMURAI day-one campaign collaboration. The present work was supported in part by a Grant-in-Aid for Scientific Research (B) (No. 22340053), and that on Innovative Areas (No. 24115005) from the Ministry of Education, Culture, Sports, Science and Technology (MEXT, Japan).

### References

- [1] Nakamura T *et al.* 1999 *Phys. Rev. Lett.* **83** 1112
- [2] Nakamura T *et al.* 2009 *Phys. Rev. Lett.* **103** 262501
- [3] Tanaka K *et al.* 2010 *Phys. Rev. Lett.* **104** 062701
- [4] Warburton E K, Becker J A and Brown B A 1990 *Phys. Rev. C* **41** 1147
- [5] Motobayashi T *et al.* 1995 *Phys. Lett. B* **364** 9
- [6] Thibault C *et al.* 1975 *Phys. Rev. C* **12** 644
- [7] Yanagisawa Y *et al.* 2003 *Phys. Lett. B* **566** 84
- [8] Doornenbal P *et al.* 2009 *Phys. Rev. Lett.* **103** 032501
- [9] Caurier E, Nowacki F, Poves A and Retamosa J 1998 *Phys. Rev. C* **58** 2033
- [10] Utsuno Y, Otsuka T, Mizusaki T and Honma M 1999 *Phys. Rev. C* **60** 054315
- [11] Hamamoto I 2012 *Phys. Rev. C* **85** 064329
- [12] Misu T, Nazarewicz W and Åberg S 1997 *Nucl. Phys. A* **614** 44
- [13] Hamamoto I 2004 *Phys. Rev. C* **69** 041306(R)
- [14] Hamamoto I 2010 *Phys. Rev. C* **81** 021304(R)
- [15] Migdal A B 1972 *Yad. Fiz.* **16** 427; English translation 1973 *Sov. J. Nucl. Phys.* **16** 238
- [16] Kobayashi N *et al.* 2012 *Phys. Rev. C* **86** 054604
- [17] Nakamura T and Kondo Y 2012 *Clusters in Nuclei* vol 2 (*Lecture Notes in Physics* vol 848), ed C Beck (Berlin: Springer) pp 67-119
- [18] Aumann T and Nakamura T 2013 *Phys. Scr.* **T152** 014012
- [19] Bertulani C and Baur G 1988 *Phys. Rep.* **163** 299
- [20] Adrich P *et al.* 2005 *Phys. Rev. Lett.* **95** 132501
- [21] Nakamura T *et al.* 1994 *Phys. Lett. B* **331** 296
- [22] Palit R *et al.* 2003 *Phys. Rev. C* **68** 034318
- [23] Fukuda N *et al.* 2004 *Phys. Rev. C* **70** 054606
- [24] Otsuka T *et al.* 1994 *Phys. Rev. C* **49** R2289
- [25] Datta Pramanik U *et al.* 2003 *Phys. Lett. B* **551** 63; Datta Pramanik U *et al.* 2002 *Prog. Theor. Phys. Suppl.* **146** 427
- [26] Nakamura T *et al.* 2009 *Phys. Rev. C* **79** 035805
- [27] Aumann T *et al.* 1999 *Phys. Rev. C* **59** 1252
- [28] Nakamura T *et al.* 2006 *Phys. Rev. Lett.* **96** 252502
- [29] Kondo Y *et al.* 2010 *Phys. Lett. B* **690** 245
- [30] Urata Y, Hagino K and Sagawa H 2011 *Phys. Rev. C* **83** 041303(R)